

Lawrence Berkeley National Laboratory

Lawrence Berkeley National Laboratory

Title

ROTATIONAL EXCITATION AND RADIATIVE LIFETIMES OF N₂⁺

Permalink

<https://escholarship.org/uc/item/6zj9n13z>

Author

Mahan, Bruce H.

Publication Date

1980-12-01



Lawrence Berkeley Laboratory

UNIVERSITY OF CALIFORNIA

Materials & Molecular Research Division

Submitted to the Journal of Chemical Physics

ROTATIONAL EXCITATION AND RADIATIVE LIFETIMES OF
 N_2^+

Bruce H. Mahan and Anthony O'Keefe

December 1980

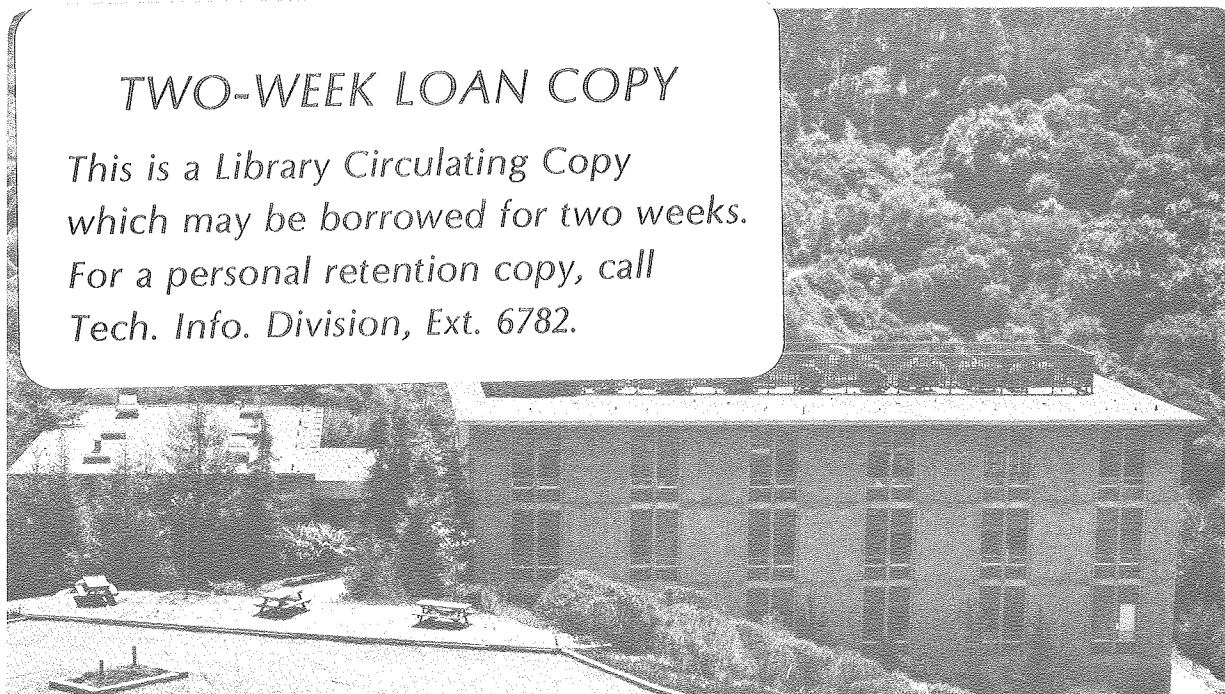
RECEIVED
LAWRENCE
BERKELEY LABORATORY

FEB 9 1981

LIBRARY AND
DOCUMENTS SECTION

TWO-WEEK LOAN COPY

*This is a Library Circulating Copy
which may be borrowed for two weeks.
For a personal retention copy, call
Tech. Info. Division, Ext. 6782.*



LBL-12026 c.2

DISCLAIMER

This document was prepared as an account of work sponsored by the United States Government. While this document is believed to contain correct information, neither the United States Government nor any agency thereof, nor the Regents of the University of California, nor any of their employees, makes any warranty, express or implied, or assumes any legal responsibility for the accuracy, completeness, or usefulness of any information, apparatus, product, or process disclosed, or represents that its use would not infringe privately owned rights. Reference herein to any specific commercial product, process, or service by its trade name, trademark, manufacturer, or otherwise, does not necessarily constitute or imply its endorsement, recommendation, or favoring by the United States Government or any agency thereof, or the Regents of the University of California. The views and opinions of authors expressed herein do not necessarily state or reflect those of the United States Government or any agency thereof or the Regents of the University of California.

ROTATIONAL EXCITATION AND RADIATIVE LIFETIMES OF N_2^+

Bruce H. Mahan and Anthony O'Keefe

Materials and Molecular Research Division
Lawrence Berkeley Laboratory and
Department of Chemistry
University of California
Berkeley, CA 94720

Abstract

The N_2^+ first negative system ($B \ ^2\Sigma_u^+ - X \ ^2\Sigma_g^+$) has been recorded by laser induced fluorescences of N_2^+ ions confined in an rf trap. The ions were produced by electron impact and had an initial rotational distribution close to the room temperature distribution of the target N_2 gas. By admitting Ar gas at pressures 10 to 100 times in excess of the N_2 pressure, variable numbers of $N_2^+ - Ar$ collisions were allowed to occur before the N_2^+ distribution was interrogated by the laser. Since the N_2^+ was translationally energetic, being driven by the trap fields, a rapid and extensive T to R energy transfer was observed. In this way, high rotational states of N_2^+ were populated and the radiative lifetimes of these states was measured. No evidence for a perturbation by a $^4\Sigma_u^+$ state was found in the region ($N = 31, 32$) where previous studies had indicated a possible perturbation. Evidence for enhanced charge transfer from $N_2^+ X \ ^2\Sigma_g^+$ to Ar was found for N_2^+ in its first vibrational level.

The high resolution spectroscopic study of molecular ions presents a great challenge to the experimentalist in that large number densities of ions are generally difficult to produce and maintain. The last few years have seen the development of several new techniques which have attempted to surmount these problems. We have recently developed a new experimental technique which combines the principles of mass spectrometry and laser induced fluorescence to produce the laser excitation spectra of mass identified molecular ions.⁽¹⁾ Our approach involves the use of a 3-dimensional quadrupole ion trap capable of storing ions in a mass selective fashion for periods of time limited only by collisional loss mechanisms. The low pressures employed in this approach allow for the determination of internal state distributions of molecular ions produced by different processes. Alternatively, the long residence time of ions permits us to alter this internal energy distribution by allowing a variable number of collisions to occur. This article describes one application of such collisional studies.

There has been a great deal of speculation in recent years as to the exact location of a predicted $4\Sigma_u^+$ state of the N_2^+ ion.^(2,3) Recent studies have reported a perturbation in the radiative lifetime of several rotational levels in the N_2^+ B $2\Sigma_u^+$ state.⁽²⁾ The observed perturbation involved a lengthening of the radiative lifetime of the $N' = 31$ and $N' = 32$ levels from 60 nsec (observed for $N' < 30$) to 69 nsec and 77 nsec, respectively. These lengthenings were not due to any identifiable perturbation by the $A^2\Pi$ State of N_2^+ and were attributed to perturbations by the long sought $4\Sigma_u^+$ state. Other groups have attempted to verify these reports by independent means, but low signal levels due to the high rotational energies involved and the low

rotational temperatures of conventional ion spectroscopy experiments have hindered these attempts. (4)

In this paper we report the careful measurement of the radiative lifetimes for all rotational components of the $B \ ^2\Sigma_u^+$ state in the area of the reported perturbation. To avoid the difficulties of low populations encountered in previous studies, we have made use of collisional heating to increase the population in the rotational levels of interest. Observed Doppler profiles for rotationally resolved transitions are consistent with a translational temperature of several thousand degrees Kelvin. The fact that the ions possess such a large velocity suggests that each collision an ion experiences with background gas molecules helps to thermalize the internal modes of the ion to a temperature of several thousand degrees. The direct electron impact ionization process of molecules generally imparts very little angular momentum to a parent ion. Thus, the collisional heating effect discussed above will be important in any excitation experiment involving energy levels not substantially populated at room temperature.

EXPERIMENTAL

For the studies reported here we employed a radio frequency ion trap of cylindrical geometry which has been described in detail elsewhere. (5) The trap consists of a hollow, cylindrical center electrode and two end caps which are electrically isolated from the center electrode and positioned at opposite ends of the cylinder, as indicated in Fig. 1. The resulting field produced by the cylindrical trap closely approximates that of a truly hyperbolic electrode arrangement which has been studied and well characterized in both experimental and

theoretical studies.⁽⁶⁾ A brief outline of the principles involved in the operation of the trap and of the relevant experimental details will be given here. A more detailed description may be found in the references already cited.

The basic principles involved are essentially those applicable to a conventional quadrupole ion lens extended to three dimensions. Application of an rf voltage to the center electrode creates a pseudo-potential in which ions are trapped regardless of their charge to mass ratio. For sufficiently high radio frequencies the resulting pseudo-potential is essentially a box within which the ions are confined. For reasons discussed below, we have utilized a relatively low frequency (~1 MHz) in order to trap a larger number of ions. This situation results in a driven rf motion of the ions which, while of small amplitude, significantly broadens the Doppler profile of the ions. While this effect makes high resolution studies difficult in general, it is still possible to observe light diatomics and triatomics with rotational resolution.

By floating the rf voltage at some dc bias level, a variable mass resolution is introduced to the trapping process which can be controlled by varying the dc to rf ratio. Variation of the peak rf voltage determines the center position of a charge to mass window such that all ions within the window are trapped, while the dc to rf ratio determines the width of the mass window. We have recently reported experiments in which a mass resolution of 1 amu was utilized at mass 14.⁽¹⁾ In the experiments reported here, low mass resolution was used since the ion studied, N_2^+ , is by far the predominant ion formed under our conditions, and no interferences were found.

Given the general design of the ion trap, the depth of the pseudo-potential well can be expressed as⁽⁷⁾

$$\bar{D} = \frac{eV^2}{4Z_0^2 Mf^2} = \frac{6.109 \times 10^{-3} V^2 \text{ volts}}{Z_0^2 Mf^2 \text{ cm amu MHz}} \quad (1)$$

Here, \bar{D} is calculated in volts, V is the maximum rf voltage between the electrodes, M is the ion mass in amu, Z_0 is half the minimum separation of the cap electrodes, and f is the applied field frequency in MHz. In the present study the values for these parameters are $Z_0 = 1$ cm, $V \approx 150$ V, $M = 28$ amu and $f = 0.5$ MHz. The corresponding well depth is 19 volts. The well depth determines the number of ions which can be trapped, since the trap reaches its maximum capacity when the space charge potential cancels the trapping potential. At this point the maximum concentration of ions is given by⁽⁷⁾

$$N_{\text{max}} \left(\frac{\text{ions}}{\text{cc}} \right) = \frac{1.66 \times 10^6 \bar{D}}{Z_0^2} \quad (2)$$

Thus for a well depth of 19 volts we find that 3×10^7 ions can be stored. From these expressions it is clear that the number of ions which may be trapped is proportional to f^{-2} . Thus, in order to trap large numbers of ions, we have used a relatively low applied frequency.

Ions are created within the trap by electron impact ionization of a selected gas (i.e., N_2 in this case) which is introduced into the vacuum chamber through a variable leak valve and maintained at a pressure of from 10^{-6} to 10^{-5} torr. The electron gun consists of a 1% thoriated 0.01" diameter tungsten filament and associated focusing electrodes. The gun is mounted in a light tight cowling attached to the center section of the ion trap and is operated in a pulsed mode,

accomplished by applying a high voltage pulse to one of the lens elements, to provide an average electron current of several μ amps. The rise time of the electron pulse using this arrangement is several μ sec.

In addition to the background gas from which the ions are formed, additional buffer gas is added in varying amounts to influence the ion-neutral collision rate in a controlled fashion. In the experiments described here Ar was used as a buffer gas at pressures varying from 0 to 10^{-3} torr (uncorrected ionization gauge). Gases of high purity (>99.9%) were used throughout this study, although the mass selectivity of the trap would permit the use of lower purity.

While the trapping potential operates continuously, the remainder of the experiment is operated in a pulsed mode at a repetition rate of 10-40 Hz. The remainder of the experiment is then most easily described by considering one experimental cycle which consists primarily of three parts: ion creation and confinement, excitation of the ions, and fluorescence signal detection.

The experiment begins with the initiation of the electron beam which creates ions for a period of several milliseconds. The electron gun is then gated off and a delay period of several hundred microseconds ensues. During these times any necessary mass selection of the ions is allowed to stabilize, and any excited electronic states which have been created are permitted to relax radiatively. Radiative relaxation of excited vibrational levels within stable electronic states is expected to be slow on the time scale of an experimental cycle. After the delay period, a 10 nsec, 1 cm^{-1} bandwidth laser pulse from a Molelectron DL-200 dye laser pumped by a Molelectron UV-1000 nitrogen laser is passed through

the ion cloud. Laser induced fluorescence is then monitored at right angles to the laser beam. A lens and mirror system directs some of the fluorescence through the wire mesh end electrodes to a cooled RCA 8575 photomultiplier tube.

In addition to fluorescence, scattered laser light may also reach the detection system. In order to minimize this background radiation, the laser beam is collimated to about 0.5 cm diameter with two lenses and directed through 0.5 meter arms (Fig. 2) containing light baffles on the entry and exit side of the trap.⁽⁸⁾ In addition to the baffle system the 10 nsec laser pulse allows the use of gated detection techniques to reduce the effects of scattered laser light.

In the present study it was convenient to block the scattered laser light reaching the PMT by means of an optical cut-off filter and observe fluorescence to the red of the excitation frequency. Since the present study involves excitation of the N_2^+ (0,0) band in the first negative system, transitions back to any higher vibration in the $X^2\Sigma$ state can be seen in this fashion. Also, since the radiative lifetime of the upper state is short, (60 nsec), almost all of the LIF occurs within tens of nsec of the laser pulse, and the elimination of all scattered laser light permits us to collect nearly all of this signal.

The signal from the RCA 8575 PMT is amplified, fed into an L.R.S. 621-BL discriminator and then to an Ortec 100 MHz counter. The counter is gated on for 200 nsec by a pulse from a photodiode triggered on the laser pulse.

After the fluorescence detection, the experimental cycle is completed by pulsing the ions out of the trap to an electron multiplier. In order to get a consistent ion signal from cycle to cycle, a high

voltage pulse must be synchronized with the rf trapping potential and applied to the bottom trap electrode. The resulting ion signal is measured by an L.R.S. 227-sg integrator and is used to normalize the fluorescence signal. The fluorescence signal is also normalized with respect to laser power which is measured by a photodiode and the gated integrator. The final signal gathered by the integrator is used to calibrate the laser wavelength. Calibration is accomplished with the use of the optogalvanic effect⁽⁹⁾ in which the laser beam is directed into a hollow cathode discharge lamp containing neon. The fluorescence excitation spectrum is then calibrated with respect to Ne^{*} transitions which are known throughout the visible region.

The timing of an experimental cycle is controlled by a series of logic circuits. The detection gates initiated by this timing circuitry are generated by Tektronix P.G. 501 pulse generators. The timing and gating logic are not shown in Fig. 2 in the interest of clarity. An on-line PDP-8f computer is responsible for the overall control of the experiment. At the end of an experimental cycle, the computer gathers the signals from the integrator and initiates a new cycle. After a predetermined number of cycles the computer retrieves the signal from the counter and advances the laser wavelength by a present increment. Typically the signal is averaged over several hundred laser pulses before advancing the wavelength. The computer normalizes the data, stores them on a disk, and produces a hard copy graph of the spectrum.

In the determination of radiative lifetimes, the experimental arrangement is modified somewhat. Control of the experimental timing is shifted from the computer to an internally controlled pulse cycle. The timing sequence is unchanged when operating in this mode, but the laser wavelength remains fixed, and the signal is collected continuously.

The output signal from the PMT is fed into a discriminator and then into a Tracor Northern NS 575 digital signal averager with a Biomation time base. This system provides a 10 nsec channel width which is suitable for the radiative decay rates encountered in the present studies. The Biomation time base is triggered by the pulse which initiates the detection gate in the normal mode of operation.

For radiative decay measurements the dye laser is tuned into resonance with a transition in the vibronic band under study. The resulting fluorescence signal as a function of time is then accumulated in the signal averager for a period of several thousand experimental cycles. The dye laser is then detuned from resonance, typically by several \AA , and a background signal is subtracted for an equivalent time period. Data from the signal averager are then transferred to a PDP-8 computer for analysis.

RESULTS AND DISCUSSION

A. Collision Dynamics

The LIF spectrum of N_2^+ ($B \ ^2\Sigma_u^+ \leftarrow X \ ^2\Sigma_g^+(0,0)$) obtained under collision free conditions is shown in Fig. 3a. The delay between the end of the 1 msec ionizing electron pulse and the laser probe pulse was 0.5 msec. Fig's 3b, c and d show the spectra obtained as successively greater amounts of Ar were introduced to the vacuum chamber while the N_2 pressure was held constant at 10^{-5} torr. While an analysis of the variation of intensity as a function of rotational level can provide an estimate of the rotational temperature of the ground state ion, care must be taken in this case to avoid lines in which members of both R and P branches overlap. (10) Examination of Fig. 3d reveals the strong

presence of P branch lines which overlap closely with members of the R branch. The presence of these lines is manifested in an apparent splitting of the R branch lines, noticeably so for lines of odd N. Under the high collision conditions used to produce the spectrum shown in Fig. 3d, it would not be unreasonable to expect the rotational population of the $X^2\Sigma_g^+$ state to be equilibrated to the temperature characteristic of the ion velocity, that is, $T_{ROT} \approx 4000-6000$ K. Clearly, since the rotational radiative relaxation times are very long compared to ion-molecule collision periods, the N_2^+ ions would thermalize to the same final characteristic temperature, regardless of buffer pressure, given enough collisions. Thus what we see in Fig's. 3a-3d are rotational-vibrational distributions, far from equilibrium with the ion translational distribution, at various stages of attainment of this equilibrium. The ability to control the collision rate allows us to freeze out the internal energy distributions and study them on a collision by collision basis.

The observed doppler width of resolved features in the spectra presented here as well as high resolution optical studies of atomic ions stored in an ion trap similar to ours⁽¹¹⁾ are consistent with the assignment of a large translational energy to the trapped ions. The actual motion of ions stored in a trap such as ours is quite complicated⁽⁶⁾ and cannot be parameterized by an equilibrium temperature. Nevertheless, we can characterize the trap conditions with a temperature equivalent which, in the present study, is on the order of 5000 K. The rate at which ions undergo collisions can be expressed by a Langevin cross section if a lower limit, corresponding to a hard sphere cross section, is observed.

The expression for the Langevin cross section is

$$\sigma_L = \pi e (2\alpha/E)^{1/2} \quad (3)$$

where e is the elementary charge, α is the polarizability of the neutral collision partner, and E is the relative collision energy. If N_2^+ has an energy of 0.42 eV ($\sim 5000^\circ K$) and the Ar is at room temperature then $\sigma_L \approx 43 \text{ \AA}^2$, which is essentially a hard sphere cross section.

The average number of collisions per second, N , which an ion undergoes is

$$N = \sigma_L \langle V_{rel} \rangle \rho \quad (4)$$

where $\langle V_{rel} \rangle$ is the average relative velocity, and ρ is the density of neutrals in the trap (which is always greater than the ion density by more than four orders of magnitude). Substituting Eq. (3) into this expression and recognizing that $\langle V_{rel} \rangle = (2E/\mu)^{1/2}$ results in the expression

$$N = 2\pi e (\alpha/\mu)^{1/2} \rho \quad (5)$$

where μ is the reduced mass of the collision partners. In the discussion of collision processes important in these experiments a convenient unit of time is 1 msec and a convenient reference density is the density at room temperature and 10^{-5} torr. Using these units, we find

$$\# N_2^+ - \text{Ar collisions/msec}/10^{-5} \text{ torr} = 0.24$$

and

$$\# N_2^+ - N_2 \text{ collisions/msec}/10^{-5} \text{ torr} = 0.27.$$

As stated earlier, the ions are created during a 1 msec period and the spectra shown in Fig. 3 are taken .5 msec following the end of

this period. Thus, each N_2^+ ion has experienced on the order of 0.3 collisions with background N_2 gas, resulting in the spectrum shown in Fig. 3a. As the Ar pressure is increased the N_2^+ ions undergo an additional 2, 10, and 20 collisions with Ar resulting in Fig's 3b through 3d, respectively. (The stated Ar pressures are uncorrected ionization gauge readings; the true pressures are approximately 80% of these readings.)

From the above discussion it is clear that N_2^+ - Ar collisions are responsible for the changes in rotational distributions observed here. While rotational excitation in the N_2^+ -Ar system has not been investigated theoretically, the N_2 -Ar system has been.⁽¹²⁾ The studies on N_2 -Ar, performed at a lower collision energy, indicate that $|\Delta N| > 2$ have appreciable cross sections and that smaller impact parameters favor successively greater ΔN 's. These results are consistent with our observations of rapid T to R energy transfer with large changes of rotational angular momentum accompanying each collision.

In addition to the (0,0) band, portions of the (1,1) band can be seen in the spectra presented here. The bandhead of the (1,1) band is indicated by an arrow in Fig. 3a. The electron impact ionization of N_2 imparts very little rotational angular momentum to the ion thus formed. In contrast, the vibrational distribution is determined by the Franck-Condon overlap of the ion with populated vibrational levels of the parent neutral. For this reason the relative populations of $v''=1$ and $v''=0$, as seen in Fig. 3a, are characterized by a temperature of several thousand degrees rather than the room temperature distribution which characterizes the initial rotational distribution.

One would then expect little or no increase in the population of $v''=1$ as a result of the energetic collisions which the N_2^+ experiences. In fact, what is observed in Fig. 3a-d is an apparent reduction in the intensity of the (1,1) band as the number of N_2^+ -Ar collisions increases. One possible cause for this effect is the spreading out of population over many rotational states in the $v''=1$ level resulting in the depletion of population in the bandhead. An alternative explanation involves the selective charge transfer from N_2^+ ($v''=1$) to Ar. The I.P. of Ar is 15.755 eV and that of N_2 is 15.576 eV. The addition of one quantum of vibrational energy ($2207 \text{ cm}^{-1} \equiv 0.274 \text{ eV}$) to N_2^+ raises its energy to 15.85 eV, thus making the charge transfer to Ar exothermic by 0.09 eV. The N_2^+ present in $v''=0$ is too low in energy to ionize Ar.

Large cross sections for charge transfer are seen in cases where the energy defect, or the difference in energy between the charge donor and the charge acceptor, is small. To test the hypothesis that rapid charge transfer is selectively depleting vibrationally excited states of N_2^+ , similar experiments were performed using Ne as the collisional partner. The ionization potential of Ne ($\sim 21.6 \text{ eV}$) is some 6 eV above ground state N_2^+ and so no effect attributable to charge transfer should be observed. The use of Ne as a collision partner results in a somewhat lower relative collision energy due to its lower mass and as a result the degree of rotational excitation of N_2^+ will be less than that found in the Ar experiments. Nevertheless, a significant amount of rotational excitation of N_2^+ was achieved (somewhat more than that observed in Fig. 3c) while the apparent intensity of the (1,1) band remained constant. Thus, it would seem that rapid charge transfer from

$N_2^+(v''=1)$ to Ar is responsible for the intensity depletion of the (1,1) band. If one assumes that all the population in $v''=1$ of N_2^+ is removed after 20 collisions with Ar (i.e., the intensity of the (1,1) band has gone to zero in Fig. 3-d) then we may estimate the cross section for charge transfer from $N_2^+(v''=1)$ to Ar as being approximately

$$\sigma_{N_2^+(v=1) \rightarrow Ar}^{C.T.} \approx \sigma_L / 20 = 2.1 \text{ \AA}^2 \quad (6)$$

B. Lifetime Measurements

The levels of spectroscopic interest are the $N = 30,31$ members of the R branch, indicated with a bracket overhead in Fig. 3c. The conditions used to measure the radiative lifetime of these levels were similar to those used to record the fluorescence excitation spectrum shown in Fig. 3c. These conditions produced a significant signal level for the lines of interest but did not appreciably populate the high P branch lines which could interfere with the measurement.

The feasibility of using the experimental arrangement described in this paper to measure radiative lifetimes has been recently demonstrated for several electronic systems in molecular ions.⁽¹³⁾ While the capability to measure radiative lifetimes ranging from 50 nsec to 10 μ sec is realizable using this arrangement, the ability to make measurements precise enough to resolve a 15 nsec difference depends on the strength of the fluorescence signal and the number of signal averager channels over which the signal is distributed. The N_2^+ B-X system is a particularly strong transition and, even when optical filters are used to reduce scattered laser light, several tens of thousands of signal photons can be collected in a short period of time. The short radiative lifetime, however, restricts the signal to perhaps 15 or 20 useable channels, thus limiting the ultimate time resolution for experi-

mentally practical collection periods. For this reason we felt it was important to demonstrate the ability to resolve such small differences under our experimental conditions. A convenient test candidate exists within the same band system under study here, being the $J = 40-45$ levels of the $B \ ^2\Sigma_u^+$ ($v=0$) state of N_2^+ . These levels are known to experience perturbations due to the $A \ ^2\Pi$ state of N_2^+ and, in addition to shifts in the line position, they are reported to possess radiative lifetimes of up to 79 nsec.⁽²⁾ Measurements of the $N = 43$ line result in an easily resolvable change of +17 nsec from the expected value of 60 nsec found in unperturbed levels. Thus we conclude that, for the electronic system studied here, a resolution of a few nsec can be easily obtained.

There are two possible mechanisms by which a perturbation between a $^4\Sigma_u^+$ state and a $^2\Sigma_u^+$ state could manifest itself; either a shift in the energy of the perturbed level (i.e., a line shift) or a sudden change in the radiative lifetime of the level could occur. High resolution studies⁽¹⁴⁾ of the N_2^+ B-X system have found no measurable perturbation in the line position for the levels $N = 30$ and 31, and an upper limit for the perturbation matrix element of 0.01 cm^{-1} has been established based on these studies.⁽¹⁵⁾ However, the amount of mixing between the two levels may still be large if they are nearly degenerate. Such mixing should be detected as a lengthening of the lifetime of the $B \ ^2\Sigma_u^+$ line.

The results we obtained for the radiative lifetimes of the $N = 30-33$ R branch lines are summarized in Table I. Typical results are presented in Fig. 4 for the R_{31} line. In all cases the signal level was quite strong and error in each determination was small relative to the magnitude of the reported perturbation. No change in the value of $\tau_{v=0}$ for the $B \ ^2\Sigma_u^+$ was detected for any level examined in this study which could be attributed to a perturbation by a $^4\Sigma$ state. This result negates the earlier measurements.⁽²⁾

SUMMARY

We have demonstrated how high rotational levels of molecular ions may be populated through collisions between energetic trapped ions and neutral species. We have used this approach to populate high rotational levels in N_2^+ allowing us to examine them for suspected perturbations in their radiative lifetime. No such perturbations were found.

ACKNOWLEDGMENTS

We are grateful to the C. B. Moore group and Linda Young for the use of and assistance with the signal averaging equipment used in this work. We thank Prof. Y. T. Lee and Prof. J. S. Winn for making useful comments and suggestions.

This research was supported by the U. S. Department of Energy, Office of Basic Energy Sciences Division of Chemical Sciences under Contract No. W-7405-Eng-48.

REFERENCES

- (1) F. J. Grieman, B. H. Mahan, A. O'Keefe, J. Chem. Phys. 72, 4246 (1980); F. J. Grieman, B. H. Mahan, A. O'Keefe, and J. Winn, Faraday Discussion No. 71, 1981.
- (2) J. Dufayard, Thesis, L'Université Scientifique et Médicale de Grenoble (1977); J. Dufayard and O. Nedelec, C. R. Acad. Sci. Ser. B285, 173 (1977); J. Dufayard, J. M. Negre, and O. Nedelec, J. Chem. Phys. 61, 3614 (1974).
- (3) M. T. Bowers, P. R. Kemper, J. B. Laudenslager, J. Chem. Phys. 61, 4394 (1974).
- (4) R. A. Gottscho and T. A. Miller, Private Communication.
- (5) See Reference 1 and references cited therein.
- (6) R. F. Bonner, J. E. Fulford, R. E. March, Int. J. Mass Spec. Ion Phys. 24, 255 (1977).
- (7) H. G. Dehmelt, Adv. Atomic and Mol. Phys. 3, 53 (1967); 5, 109 (1969).
- (8) J. G. Pruett and R. N. Zare, J. Chem. Phys. 64, 1774 (1976).
- (9) D. S. Ling and P. K. Schenck, Laser Focus, March, 60 (1978).
- (10) J. H. Moore, Jr. and J. P. Doering, Phys. Rev. 174, 178 (1968).
- (11) R. D. Knight, and M. H. Prior, J. Appl. Phys. 50, 3044 (1979).
- (12) M. D. Pattengill, J. Chem. Phys. 62, 3137 (1975); R. T. Pack, J. Chem. Phys. 62, 3134 (1975) and references therein.
- (13) B. H. Mahan and A. O'Keefe, in preparation.
- (14) K. A. Dick, W. Benesch, H. M. Crosswhite, S. G. Tilford, R. A. Gottscho, and R. W. Field, J. Molec. Spec. 69, 95 (1978).
- (15) R. A. Gottscho, Private Communication.

Table I

Experimental radiative lifetimes for
selected rotational levels of $N_2^+ B^2\Sigma_u^+$

<u>N'</u>	<u>Lifetime (nsec)</u>
30	58
31	60
32	60
33	62
42	79
43	77

FIGURE CAPTIONS

- Figure 1. Schematic representation depicting a vertical slice of the quadrupole ion trap used in the present study. A radio frequency voltage is applied to the center ring electrode while the top and bottom electrodes are maintained at ground potential. Ions, spacially confined to the enclosed region, possess a nearly Gaussian density distribution peaking at the center of the trap.
- Figure 2. Experimental arrangement used in the frequency scanning experiments. The depicted arrangement and timing sequence are discussed in the text.
- Figure 3. LIF spectra of $N_2^+ B^2\Sigma_u^+ - X^2\Sigma_g^+$ (0,0) band. Figures a, b, c, and d show the rotational distribution of N_2^+ after 0, 2, 10, and 20 collisions respectively. The arrow in Fig. (a) denotes the (1,1) band head.
- Figure 4. Log of the LIF intensity as a function of time for $N' = 33$ of $N_2^+ B^2\Sigma_u^+$.

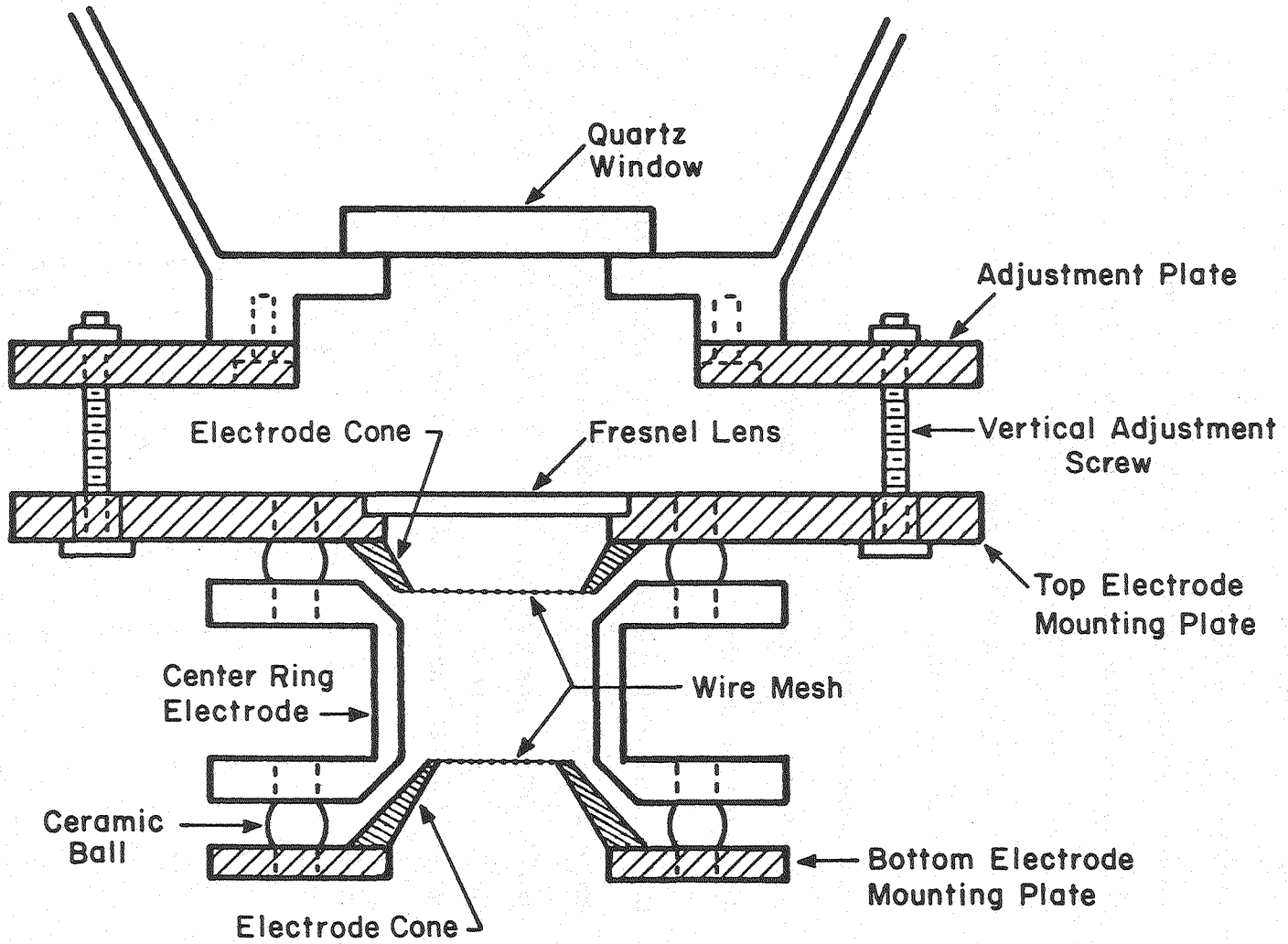


Figure 1

XBL 798-11079

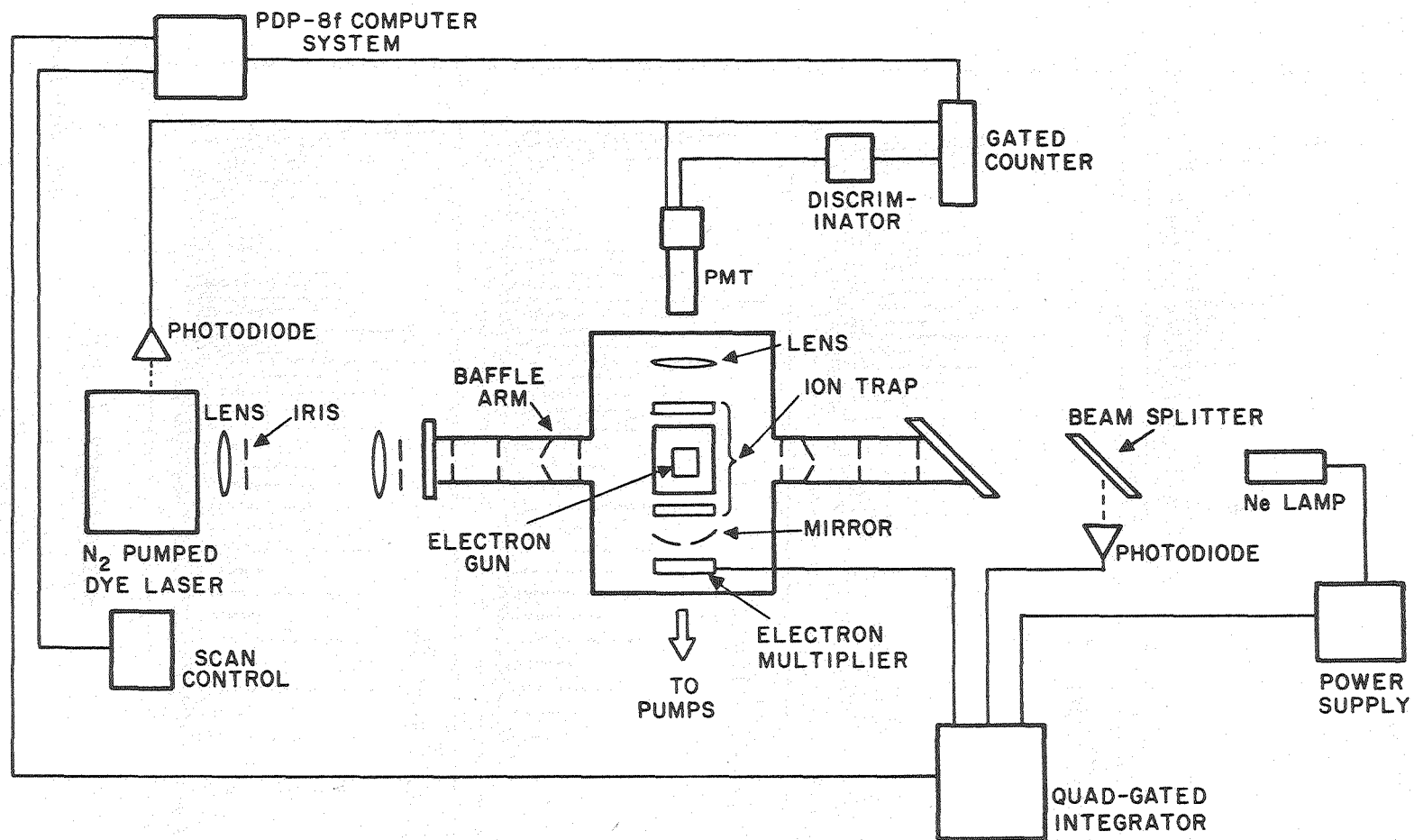
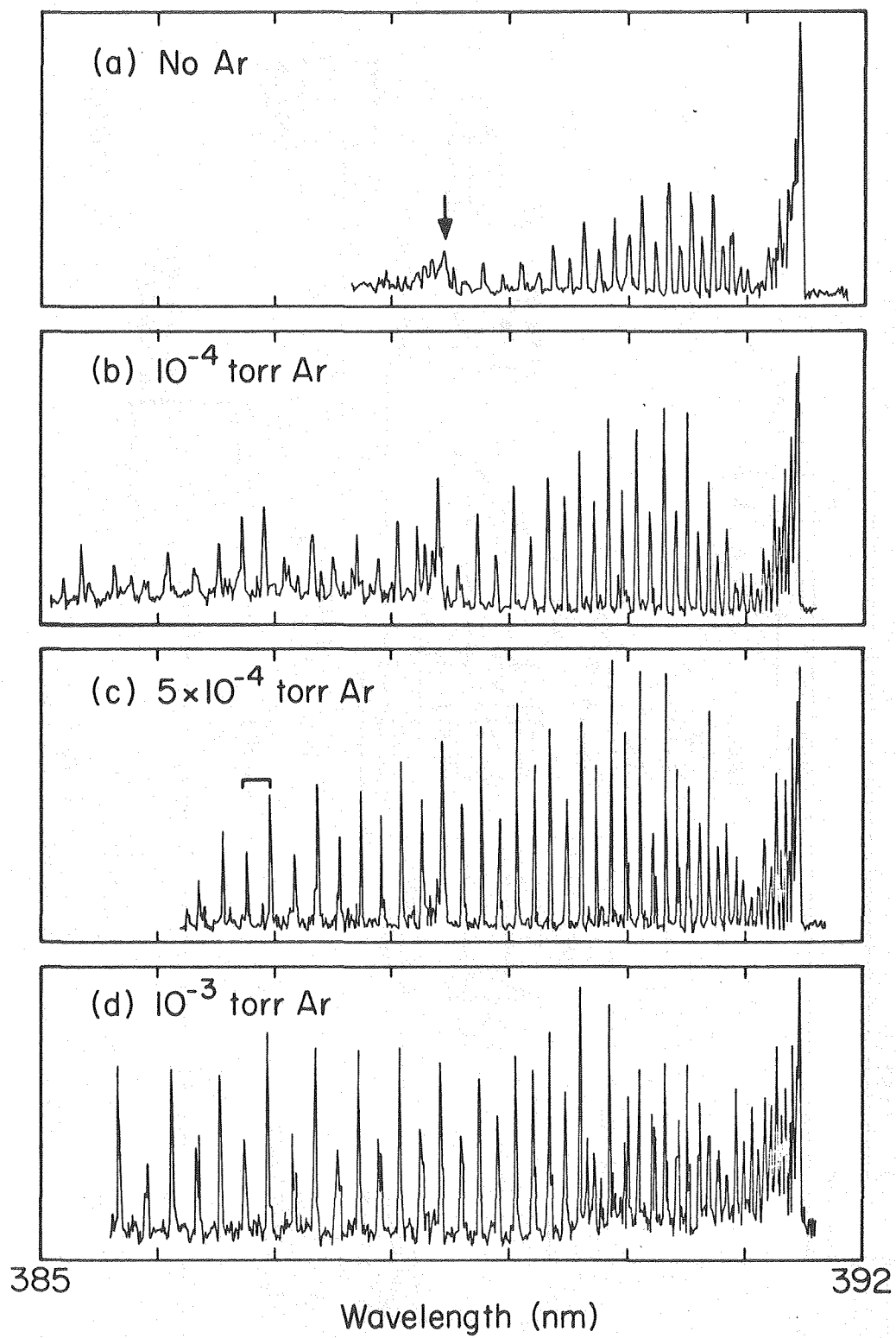


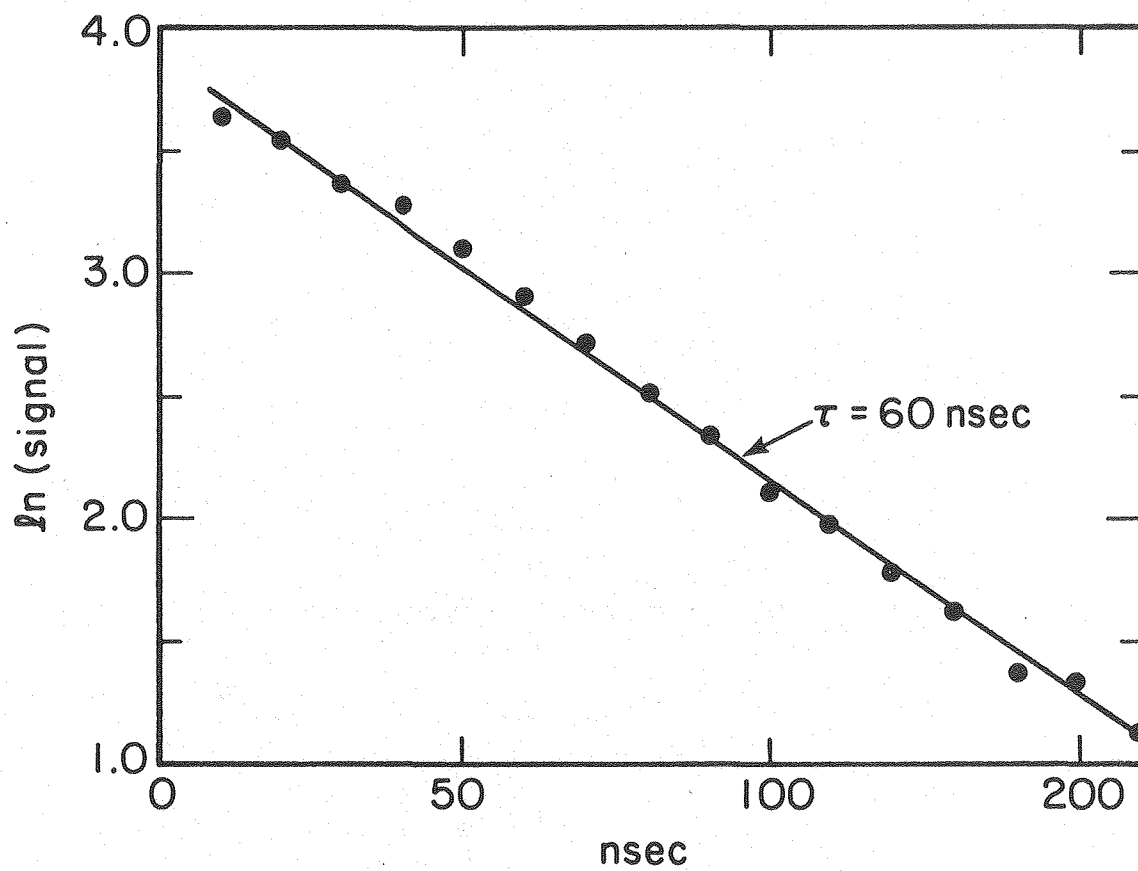
Figure 2

XBL 807-10716



XBL 8011-7450

Figure 3



XBL 8011-7449

Figure 4

